

PRECLINICAL REPORTS

Clinical endpoints of needle-free jet injector treatment: An in depth understanding of immediate skin responses

Liora Bik MD¹  | Martijn B. A. van Doorn MD, PhD¹  | Neill Boeijink MD² |
 Medelyn Wennekers MD¹ | Arne A. Meesters MD, PhD² |
 Peter Bloemen MD, PhD, DMSc³ | Merete Haedersdal MD, PhD, DMSc⁴  |
 Albert Wolkerstorfer MD, PhD² 

¹Department of Dermatology, Erasmus MC University Medical Center Rotterdam, Rotterdam, The Netherlands

²Department of Dermatology, Amsterdam UMC Medical Center, Amsterdam, The Netherlands

³Department of Biomedical Engineering, Amsterdam UMC Medical Center, Amsterdam, The Netherlands

⁴Department of Dermatology, Bispebjerg Hospital, University of Copenhagen, Copenhagen, Denmark

Correspondence

Liora Bik, MD, Department of Dermatology, Erasmus MC University Medical Center Rotterdam, Doctor Molewaterplein 40, 3015 GD Rotterdam, The Netherlands.
 Email: l.bik@erasmusmc.nl

Abstract

Objectives: Needle-free jet injectors have been used in dermatological practice for many years. However, predefined clinical endpoints that guide physicians to choose optimal device settings have not been clearly defined. Here, we evaluate immediate skin responses as clinical endpoints for needle-free jet injector treatments.

Methods: We injected methylene blue in ex vivo human skin using an electronically-controllable pneumatic injector (EPI; 3–6 bar, 50–130 μ l; $n = 63$), and a spring-loaded jet injector (SLI) with fixed settings (100 μ l; $n = 9$). We measured the immediate skin papule (3D-camera), residual surface fluid (pipette), dermal dye distribution by estimating depth and width, and subcutaneous dye deposition.

Results: EPI with 4 bar and 100 μ l resulted in the largest skin papule of 48.7 mm³ (35.4–62.6 mm³) and widest dermal distribution of 8.0 mm (5.5–9.0 mm) compared to EPI with 6 bar and 100 μ l ($p < 0.001$, $p = 0.018$, respectively). The skin papule volume showed a significant moderate to high positive correlation with the width and depth of dye distribution in the dermis ($r_s = 0.63$, $r_s = 0.58$, respectively; $p < 0.001$ for both correlations). SLI showed high variability for all outcome measures. Finally, a trend was observed that a small skin papule (≤ 7 mm) and little residual surface fluid ($\leq 10\%$ of injection volume) were warning signs for subcutaneous deposition.

Conclusions: The immediate skin papule and residual surface fluid correspond with dermal drug deposition and are relevant clinical endpoints for needle-free jet injector treatments in dermatological practice.

KEYWORDS

dermatology, drug delivery, injection, intralesional, jet injection, needle-free injection, pneumatic injection

INTRODUCTION

Needle-free jet injectors have been used for over 75 years for the transdermal delivery of vaccines, insulin and for the treatment of dermatological indications such as hypertrophic

scars, keloids, and warts.¹ By producing a high-powered jet stream of fluids, jet injectors are able to penetrate the epidermis providing dermal drug delivery without the use of (painful) needles. Advantages of jet injectors include the fast-working mechanism, standardized injections, absent risk of

This is an open access article under the terms of the Creative Commons Attribution-NonCommercial-NoDerivs License, which permits use and distribution in any medium, provided the original work is properly cited, the use is non-commercial and no modifications or adaptations are made.

© 2022 The Authors. *Lasers in Surgery and Medicine* published by Wiley Periodicals LLC

needle-stick injuries, and nearly pain-free delivery of fluids into the skin. Disadvantages of jet injector systems might include clogging of the nozzle, splash back, need for sterilization of the device after each patient, and non-adjustable settings. Since the introduction of the first jet injector in the 1960s, novel (electronically powered) jet injector systems have been developed to overcome most of these drawbacks.

Jet-injectors can mainly be classified into two groups: (a) spring-loaded jet injectors (SLI) and (b) gas/air-powered jet injectors.² Traditional SLI operate with a spring mechanism, which is manually charged for every injection, and released by triggering the device which induces a jet-stream. Device settings are usually fixed and non-tuneable. Electronically-controlled pneumatic jet injectors (EPI) are novel air-powered jet injectors that, in contrast to SLI, operate with tuneable pressure and injection volume settings to create tailor made treatments for dermal drug delivery.

Needle-free jet injectors induce immediate skin responses that are directly visible after each injection. This jet-tissue interaction, such as skin elevation and residual surface fluid, are potential clinical endpoints that may serve as indicators of dermal drug delivery. Close observation of the clinical endpoints can be a useful tool for selecting optimal device settings for each patient and/or anatomical location. To date, however, predefined clinical endpoints that relate to dermal drug delivery of jet injectors have not been defined. Therefore, we aimed to evaluate immediate skin responses as clinical endpoints for spring- and air-powered needle-free jet injector treatments.

MATERIALS AND METHODS

Study design

In this ex vivo human skin study, jet injector induced immediate skin responses including skin papule formation, postinjection residual surface fluid and dermal dye distribution, were explored using two types of jet injectors. Needle injections were included for comparison. Skin papule dimensions were captured with a 3D camera system, and postinjection residual surface fluid was extracted and measured using a pipette. Dermal distribution dimensions were analysed by estimating depth and width of the dye staining following excision of skin tissue.

The Ethics Board Committee of Amsterdam UMC concluded that this study with ex vivo human tissue was exempted from formal approval because of no risk to participants and the use of anonymous tissue.

Skin preparation

Freshly excised human skin was anonymously obtained from three patients during elective abdominoplasty

(Department of Plastic Surgery; OLVG Hospital). Excessive adipose tissue was removed until a skin thickness (including subcutaneous layer) of 2 cm remained, and the specimen was subsequently stored at -20°C up to 8 weeks. Before start, the tissue was thawed at room temperature, fixated under light tension, and marked with 2×2 cm test zones.

Interventions and sample collection

EPI was performed with an electronically-controlled pneumatic jet injector (EnerJet2.0; PerfAction Technologies Ltd.) at 3, 4, 5, and 6 bar, (100 μl ; $n = 36$), and injection volumes of 50, 100, and 130 μl (4 bar; $n = 27$). The EPI nozzle tip (\varnothing 0.2 mm) has a 5 mm distance to the skin surface, determined by the spacer. A spring loaded jet-injector (Dermojet; AKRA) with a fixed pressure of 98 bar and injection volume of 100 μl was selected for SLI ($n = 9$).² One researcher (MW) delivered a constant intradermal bolus of 100 μl by conventional needle injection with a 0.5 ml syringe with 29 G needle ($n = 9$, BD Micro-Fine, 324892; Becton Dickinson). All injections with normal saline containing 0.1% of methylene blue (C.I. 52015; Merck Millipore) were divided over three different human tissue specimens and performed in triplicate to minimize bias due to variation in physical skin properties. Undelivered liquid on the skin was defined as residual surface fluid, and collected and measured using a lab pipette (0.5–10 μl ; 10–100 μl). The skin papule border was manually contoured using a black marker for 3D analyses. Photographs were captured by digital camera (D5300; Nikon), and a 3D camera system (Antera 3D[®] CS; Miravex Limited) under standardized conditions including normal room lighting, fixed distance and perpendicular angle. Each skin papule was linearly incised directly at the entry point of injection, removed (2 cm \times 1 cm), and mounted under slight pressure between two microscopic slides with the injection site facing upwards. A ruler was used for measurements of the immediate cutaneous distribution by two trained assessors (AM & AW) who measured the maximum dermal width and depth (dermis only), and the presence of dye deposition into the subcutaneous layer.

3D-system assessment of the skin papule

Antera 3D[®] CS (Miravex Limited) operates by multi-directional illumination of LEDs at different wavelengths, and was used to capture the skin papule immediately after each injection. The contour of the skin papule was selected as field of interest for assessment of the skin papule volume (mm^3) and diameter (mm) in the corresponding software (Mode: elevation, Filter: extra-large).

Statistics

Descriptive data were presented as median and interquartile ranges (IQR; Q1–Q3). Outliers were included after comparing groups with and without outliers using Mann–Whitney U test ($p > 0.05$). The correlation coefficient between the skin papule volume and dermal distribution was measured with Spearman's rho for nonparametric correlations. Equality of EPI subgroups in papule volume, dermal distribution and residual surface fluid was explored using Kruskal–Wallis test. Since all tested outcome measures showed inequality ($p < 0.05$), additional comparisons using Mann–Whitney U test were performed. Comparisons were limited to two EPI subgroups with the highest numerical differences for pressure and injection volume. Formal correction for multiple testing was therefore not required. The χ^2 test was used for comparison of the risk of subcutaneous dye deposition following jet injection. An α level of 5% was applied. Analyses were performed in SPSS version 25 (IBM Corporation).

RESULTS

Jet injection induced skin papule

The skin papule formation was evaluated immediately after injection for all interventions by 3D-camera (Figures 1 and 2; Table 1). For EPI, we compared different pressures while using a constant injection volume of 100 μL . EPI with 4 bar resulted in the largest skin papule with a volume of 48.7 mm³ (35.4–62.6 mm³) and a diameter of 9.8 mm (8.8–11.2 mm), compared to the smallest skin papule for EPI with 6 bar with a volume of 11.9 mm³ (4.6–26.9 mm³; $p < 0.001$) and diameter of 6.1 mm (5.1–8.1 mm; $p = 0.018$). When comparing different injection volumes while using a constant pressure of 4 bar, EPI with 100 μL resulted in the largest skin papule with a volume of 48.7 mm³ (35.4–62.6 mm³) and diameter of 9.8 mm (8.8–11.2 mm), compared to 50 μL with a small papule volume of 12.8 mm³ (5.5–21.0 mm³; $p < 0.001$) and diameter of 6.5 mm (6.1–8.1 mm; $p = 0.020$). For SLI, we observed a large variation

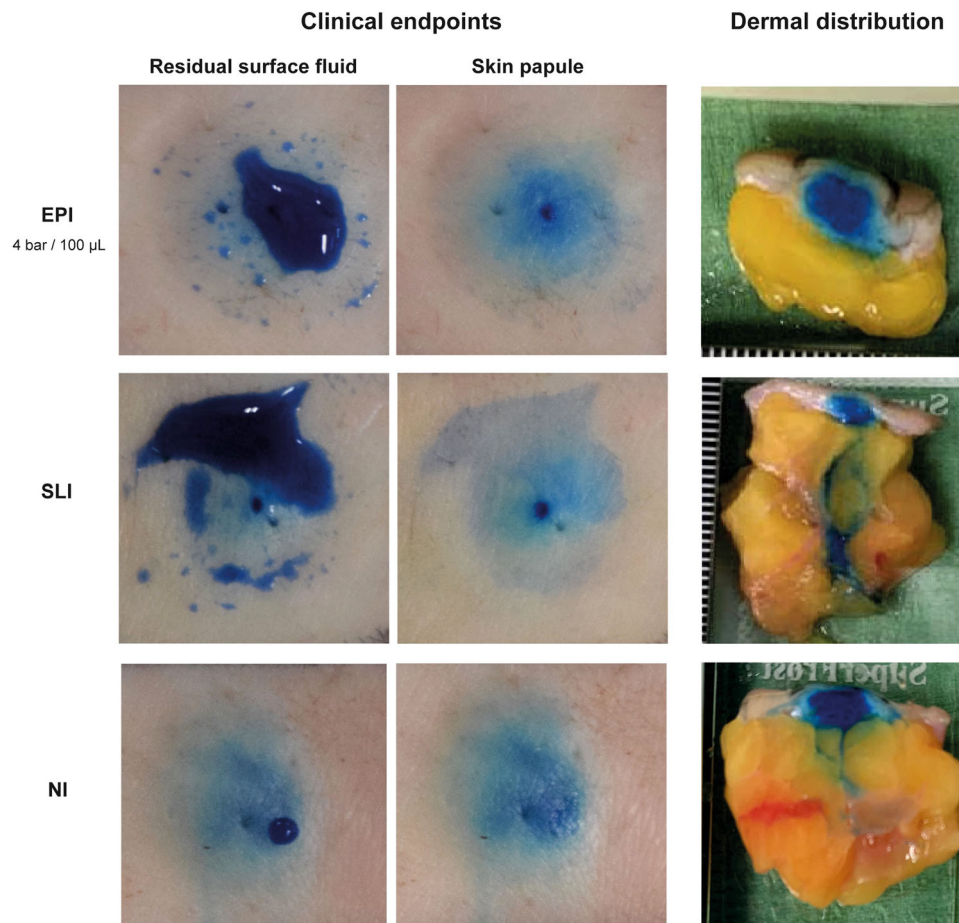


FIGURE 1 Residual fluid on skin surface and the immediate skin papule are clinical endpoints of needle-free jet injector treatments, and relate to the intradermal spatial dye distribution. Needle injection served as control. EPI, electronic pneumatic injection; NI, needle injection; SLI, spring-loaded jet injection

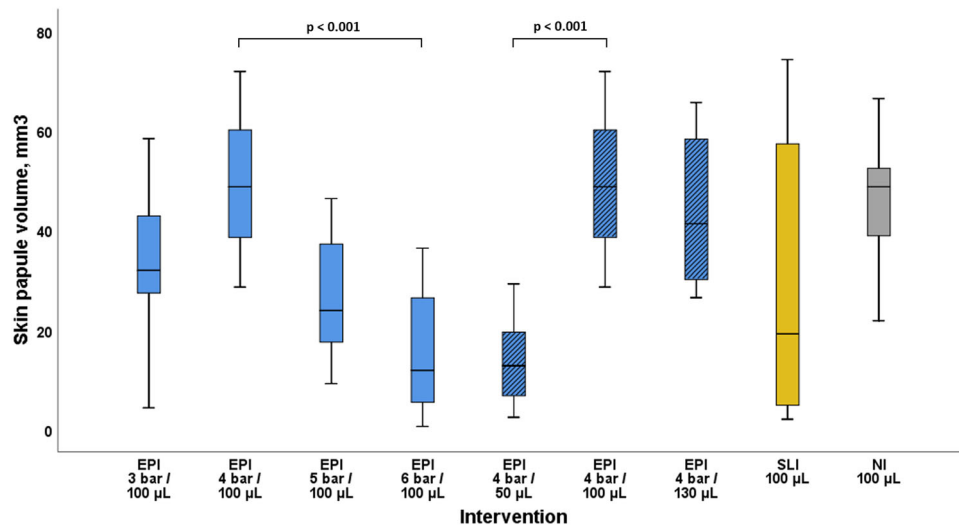


FIGURE 2 Boxplot presenting the median and interquartile ranges with min/max whiskers of the skin papule volume in mm^3 for all interventions. EPI with 4 bar and $100\ \mu\text{L}$ resulted in the largest immediate skin papule. High variability in skin papule volume was observed for SLI. Needle injection served as control. EPI with 4 bar and $100\ \mu\text{L}$ is presented in duplicate. EPI, electronic pneumatic injection; NI, needle injection; SLI, spring-loaded jet injection

between single injections resulting in a small median papule volume of $19.2\ \text{mm}^3$ ($4.1\text{--}60.4\ \text{mm}^3$) and a diameter of $7.0\ \text{mm}$ ($6.8\text{--}12.8\ \text{mm}$). Intradermal needle injection served as control and resulted in a papule volume of $48.7\ \text{mm}^3$ ($36.6\text{--}56.3\ \text{mm}^3$), and a diameter of $10.7\ \text{mm}$ ($10.7\text{--}11.7\ \text{mm}$).

Jet injection induced residual fluid on skin surface

Directly after injection, residual fluid on the skin surface was observed for all interventions and collected using a pipette (Figures 1 and 3; Table 1). EPI with 5 bar and $100\ \mu\text{L}$ resulted in the lowest residual surface fluid volume of $9.5\ \mu\text{L}$ ($7.7\text{--}15.7\ \mu\text{L}$), compared to EPI with 3 bar and $100\ \mu\text{L}$ with a residual surface volume of $18.7\ \mu\text{L}$ ($11.7\text{--}30.8\ \mu\text{L}$; $p = 0.053$). When comparing the different injection volumes of EPI, injections with $130\ \mu\text{L}$ left a residual surface fluid volume of $12.6\ \mu\text{L}$ ($9.9\text{--}19.8\ \mu\text{L}$), corresponding to 9.3% of its injection volume. Smaller injection volumes of $100\text{--}50\ \mu\text{L}$ led to an increase in the residual fluid percentage. SLI with $100\ \mu\text{L}$ resulted in a residual fluid volume of $16.0\ \mu\text{L}$ ($6.2\text{--}26.5\ \mu\text{L}$; 16.0%). Needle injections with $100\ \mu\text{L}$ resulted in a limited residual fluid volume of only $0.6\ \mu\text{L}$ ($0.5\text{--}1.5\ \mu\text{L}$; 0.6%).

Jet injection induced dermal dye distribution

The immediate dermal dye distribution dimensions are shown in Figures 1 and 4A,B, and in Table 1. EPI with 4 bar and $100\ \mu\text{L}$ resulted in the largest dermal distribution dimensions with a dermal width of $8.0\ \text{mm}$

($5.5\text{--}9.0\ \text{mm}$) and dermal depth of $5.0\ \text{mm}$ ($4.0\text{--}6.0\ \text{mm}$), compared to EPI with 6 bar and $100\ \mu\text{L}$ with the smallest dimensions with a dermal width of $5.0\ \text{mm}$ ($3.5\text{--}6.0\ \text{mm}$; $p = 0.018$) and dermal depth of $3.0\ \text{mm}$ ($2.5\text{--}5.0\ \text{mm}$; $p = 0.059$). Comparing different injection volumes, EPI with 4 bar and $100\ \mu\text{L}$ resulted in the largest dermal distribution (dimensions stated above), compared to EPI with 4 bar and $50\ \mu\text{L}$ with a small dermal width of $4.5\ \text{mm}$ ($3.0\text{--}6.0\ \text{mm}$; $p = 0.009$) and dermal depth of $3.0\ \text{mm}$ ($1.8\text{--}4.5\ \text{mm}$; $p = 0.147$). SLI resulted in small dermal distribution, and high inter-injection variance, with a dermal width of $4.0\ \text{mm}$ ($2.5\text{--}8.0\ \text{mm}$), and a dermal depth of $4.0\ \text{mm}$ ($2.5\text{--}5.5\ \text{mm}$). For needle injections, we observed a dermal distribution with a width of $6.0\ \text{mm}$ ($5.0\text{--}6.0\ \text{mm}$) and a depth of $3.0\ \text{mm}$ ($2.0\text{--}4.0\ \text{mm}$). Dermal thickness of the three skin samples was $5.0\ \text{mm}$ ($4.0\text{--}5.0\ \text{mm}$) measured before intervention, similar as reported in previous studies, and differ not significantly from each other.³ Measured dermal depth distribution of $>5.0\ \text{mm}$ was caused by swelling/expansion of the dermis by the injected fluid volume.

Overall, a significant moderate to high positive correlation was observed for the skin papule volume and the dermal distribution in width ($r_s = 0.63$; $p < 0.001$), and papule volume and dermal distribution in depth ($r_s = 0.58$; $p < 0.001$).

Jet injection induced subcutaneous deposition

After excision, deep dye distribution reaching the subcutaneous tissue was observed for a subset of the skin samples for all interventions (Table 1). For EPI with 5 bar and $100\ \mu\text{L}$, subcutaneous dye deposition was

TABLE 1 Overview of the needle-free jet injector induced immediate skin responses

Injection technique	Skin papule		Residual surface fluid		% of injection volume		Dermal dye distribution		Subcutaneous deposition	
	Volume in mm ³ , (Q1–Q3)	Diameter in mm, (Q1–Q3)	Volume in µl, (Q1–Q3)	Diameter in mm, (Q1–Q3)	Volume in µl, (Q1–Q3)	% of injection volume	Width in mm, (Q1–Q3)	Depth in mm, (Q1–Q3)	Number of samples, (%) ^a	
EPI										
100 µl/3 bar ^{b,c}	31.9 (21.8–47.7)	9.8 (8.1–11.2)	18.5 (11.7–30.8)	9.8 (8.1–11.2)	18.5 (11.7–30.8)	18.5%	6.0 (5.0–7.0)	3.0 (2.5–4.0)	1 (11%)	
100 µl/4 bar	48.7 (35.4–62.6)	9.8 (8.8–11.2)	15.2 (13.2–20.3)	9.8 (8.8–11.2)	15.2 (13.2–20.3)	15.2%	8.0 (5.5–9.0)	5.0 (4.0–6.0)	2 (22%)	
100 µl/5 bar	23.9 (13.7–41.3)	7.0 (7.0–8.8)	9.5 (7.7–15.7)	7.0 (7.0–8.8)	9.5 (7.7–15.7)	9.5%	6.0 (5.0–7.3)	4.0 (3.5–5.0)	9 (100%)	
100 µl/6 bar	11.9 (4.6–26.9)	6.1 (5.1–8.1)	10.8 (7.9–13.4)	6.1 (5.1–8.1)	10.8 (7.9–13.4)	10.8%	5.0 (3.5–6.0)	3.0 (2.5–5.0)	8 (89%)	
50 µl/4 bar	12.8 (5.5–21.0)	6.5 (6.1–8.1)	9.8 (7.5–13.3)	6.5 (6.1–8.1)	9.8 (7.5–13.3)	19.6%	4.5 (3.0–6.0)	3.0 (1.8–4.5)	2 (22%)	
100 µl/4 bar	48.7 (35.4–62.6)	9.8 (8.8–11.2)	15.2 (13.2–20.3)	9.8 (8.8–11.2)	15.2 (13.2–20.3)	15.2%	8.0 (5.5–9.0)	5.0 (4.0–6.0)	2 (22%)	
130 µl/4 bar	41.3 (29.0–59.4)	11.7 (9.1–11.7)	12.6 (9.9–19.8)	11.7 (9.1–11.7)	12.6 (9.9–19.8)	9.3%	7.0 (7.0–8.0)	4.0 (4.0–5.0)	5 (56%)	
SLI										
100 µl	19.2 (4.1–60.4)	7.0 (6.7–12.8)	16.0 (6.2–26.5)	7.0 (6.7–12.8)	16.0 (6.2–26.5)	16.0%	4.0 (2.5–8.0)	4.0 (2.5–5.5)	5 (56%)	
NI										
100 µl	48.7 (36.6–56.3)	10.7 (10.7–11.7)	0.6 (0.5–1.5)	10.7 (10.7–11.7)	0.6 (0.5–1.5)	0.6%	6.0 (5.0–6.0)	3.0 (2.0–4.0)	2 (22%)	

Note: EPI with 4 bar and 100 µl is presented in duplicate.

Abbreviations: EPI, electronic pneumatic injection; NI, needle injection; SLI, spring-loaded jet injection.

^aTotal per group: $N = 9$.

^bInjection volume.

^cDriving pressure.

Residual surface fluid

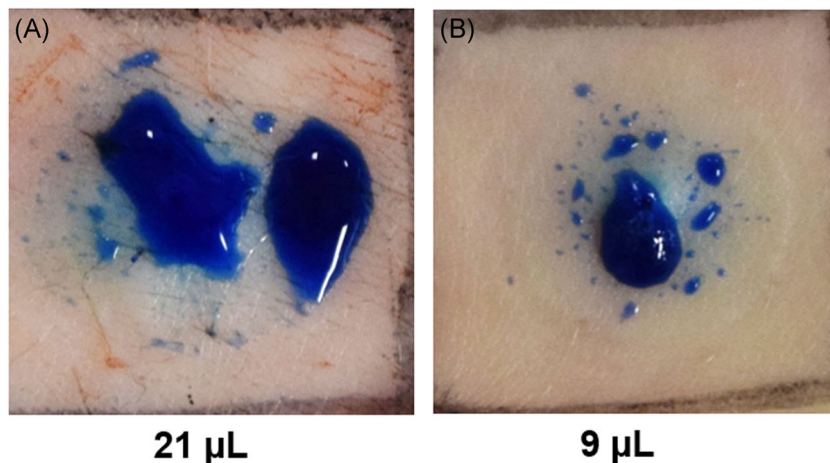


FIGURE 3 Representative clinical photographs of the residual surface fluid as clinical endpoint after injection with an electronically-controllable pneumatic injector (EPI) with methylene blue dye (blue). (A) High residual surface fluid volume of 21 μL after EPI with 3 bar and 100 μL , which is visually distinguishable from (B) with a low residual surface fluid volume of 9 μL after EPI with 6 bar and 100 μL

observed in all samples (100%), while this was only observed in one sample for EPI with 3 bar and 100 μL (11%; $p < 0.001$). Moreover, a trend was observed for subcutaneous dye deposition when using a high injection volume of 130 μL (56%), compared to a low injection volume of 50 μL (22%, $p = 0.147$). For SLI, subcutaneous deposition was observed in 54% of the injections. For needle injections, only 22% of the injections resulted in subcutaneous dye deposition, which was similar to EPI with a low pressure level (4 bar).

DISCUSSION

In this ex vivo human skin study, the clinical endpoints of spring- and air-powered needle-free jet injector systems were assessed by evaluating their immediate skin responses. Our results suggest that the immediate skin papule and residual surface fluid on the skin surface are useful clinical endpoints, which closely correspond with the intradermal spatial dye distribution. A relatively small skin papule and little residual surface fluid, however, could act as warning sign for deep distribution into subcutaneous tissue. Of all tested EPI settings, 4 bar and 100 μL resulted in the highest intradermal dye deposition. For SLI, we observed intradermal drug deposition with high variability between single injections.

In dermatological practice, immediate clinical endpoints are commonly used to indicate therapeutic response or risk for complications.⁴ Well-known examples in laser dermatology are the whitening response from Q-switched lasers and the purpura from pulsed dye lasers. With jet injectors, such endpoints have not been investigated systematically. In this study, we found that the immediate formation of a skin papule is a good clinical endpoint that indicates delivery of the fluid into the dermis. Moreover, EPI with 4 bar and 100 μL resulted in the largest skin papule volume and most extensive dermal deposition in

width and in depth. Both higher and lower EPI pressure settings, or SLI with fixed settings, resulted in a smaller skin papule size, and corresponding decreased dermal deposition. We previously reported a similar relation between the papule size and dermal dispersion, however, with no difference between EPI at 4 or 6 bar pressure, in ex vivo pig skin.⁵ This could be explained by the small injection volume of 50 μL that was injected in thicker and more resilient pig skin tissue in the previous study. Erlendsson et al. investigated the dermal dispersion pattern of EPI, using the same jet injector system as in our study, at 3.1, 3.9, and 4.6 bar pressure and 80 μL injection volume in ex vivo pig skin, and found that dermal depth was influenced by the pressure level, while the dermal width increased by stacking of single injections.⁶ However, they did not measure the skin papule dimensions or volume of residual surface fluid on the skin. Simmons et al quantified skin reactions after SLI in ex vivo guinea pig skin, and reported a positive correlation between the dye dispersion diameter from a transsectional side-view and the injection volume.⁷

Besides the skin papule, the residual fluid on the skin surface also appears to be a relevant clinical endpoint, especially for the risk of infiltration into the subcutaneous tissue when aiming for a dermal target. We found that a combination of a relatively small residual surface fluid ($\leq 10\%$ of injected volume) and a small papule (≤ 7 mm in diameter) relates to a high risk of subcutaneous infiltration, mostly seen after EPI at higher pressures (5 and 6 bar) and SLI (98 bar). The sole use of residual surface fluid as clinical endpoint for subcutaneous deposition is insufficient. We assume that beyond a certain pressure level, the kinetic energy of the fluid is high enough to cross the dermis and deliver fluid primarily into the subcutaneous tissue. The injection volume was also found to be an important factor for the location of drug deposition; EPI with a larger volume of 130 μL resulted more frequently in subcutaneous infiltration. In addition, residual

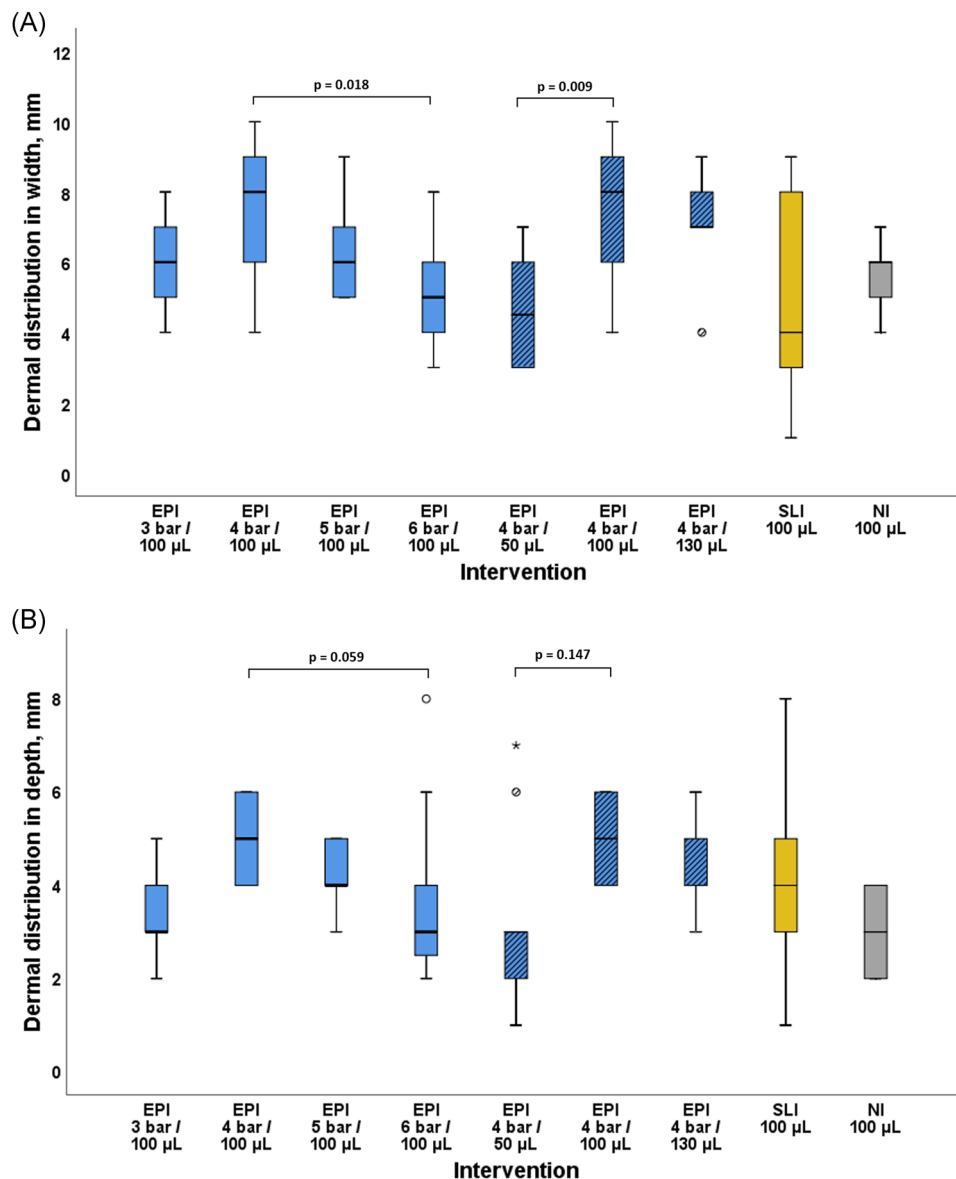


FIGURE 4 (A, B) Boxplots presenting the median and interquartile ranges with min/max whiskers of needle-free jet injector induced dermal dye distribution in width (A) and depth (B) for all interventions. EPI with 4 bar and 100 µL resulted in the largest dermal distribution. SLI showed high variability for intradermal dye distribution in depth and width. Needle injection served as control. The boxplot includes outliers and EPI with 4 bar and 100 µL is presented in duplicate. EPI, electronic pneumatic injection; NI, needle injection; SLI, spring-loaded jet injection

fluid on the skin surface is also relevant for environmental drug contamination and the cumulative drug dosage, especially when chemotherapeutic agents are being used. Besides, it is important to realize that the physical properties of the skin vary with dermal thickness, age, body mass index, ethnicity, gender, and anatomical location, which may all influence the drug distribution. Therefore, based on clinical endpoints, optimal jet injector settings should be adjusted for every individual patient, skin condition and anatomical location.^{8,9}

Since the introduction of the first jet injector in the early twentieth century, spring- and gas-/air-powered jet injectors were developed to deliver substances into the skin. Advantages of SLI devices include their compactness, low cost

and high durability, while disadvantages include fixed settings, need of sterilization between patients, and higher risk of (unwanted) subcutaneous drug deposition.¹ EPI devices have the advantage of a reliable injection force, greater flexibility in device settings, and disposable nozzle tips to provide continuation of patients care. Their disadvantages include the use of an exhaustible gas source (for gas-powered jet injectors operating with gas [usually CO₂] cartridges), and higher cost.

In clinical practice, jet injectors are mainly used for intradermal drug administration of topical corticosteroids in keloids, hypertrophic scars and inflammatory disorders. A growing, but unregulated grey area, is the jet injection of hyaluronic acid for skin rejuvenation by

non-physicians. Other, more specialized indications are the delivery of bleomycin in common warts, anaesthetics for local pain management, botulinum toxin for hyperhidrosis, and 5-aminolevulinic acid for photodynamic therapy.^{10–15} Jet injectors can also be directed to target the subcutaneous tissue, for example, for administration of biologicals, vaccines, insulin, and nicotine.^{16–19} The parameters of the currently available jet injector systems, however, needs to be optimized to adequately deliver larger volumes.

Limitations of this study include the use of an ex vivo human skin model to mimic an in vivo clinical setting. Although we expect that the correlation between jet injector settings on the clinical endpoints and dermal distribution in ex vivo skin will most likely be the similar to an in vivo setting, a formal evaluation of clinical endpoints in in vivo skin has yet to be performed. In addition, the use of abdominal skin from three obese patients that was partially affected by stretch marks potentially altering the distribution patterns. However, by performing all measurements in triplicate for each of the three patients, we could minimize the effect of outliers. In addition, only two of many available jet injectors were evaluated, and fluids with a different viscosity may lead to different results. Lastly, the residual surface fluid was measured with a lab pipette, which is unpractical in clinical practice. The researcher, however, were able to visually distinguish low and high residual surface fluid volumes during the course of the study (Figure 4). We suggest operators to first gain experience with the device settings and visually distinguishing surface fluid volumes to correctly use this clinical endpoint, in combination with the skin papule, in daily clinical practice.

For future research, we suggest to investigate the effect of jet injection induced skin responses at different anatomical sites, differences in age of the patient and skin lesions with other mechanical properties like various forms of scar tissue.

CONCLUSION

In conclusion, our results suggest that the immediate skin papule and residual fluid on the skin surface are relevant clinical endpoints for spring- and air-powered needle-free jet injector systems in normal human skin. These endpoints are indispensable for the successful and safe treatment with needle-free jet injector systems in clinical practice.

ACKNOWLEDGMENTS

We thank J. Florisson and G. Krebbers for their contribution to this study.

CONFLICT OF INTERESTS

The EnerJet device was provided by PerfAction as part of a research collaboration.

ORCID

Liora Bik  <http://orcid.org/0000-0002-4624-5383>

Martijn B. A. van Doorn  <http://orcid.org/0000-0003-1672-7899>

Merete Haedersdal  <http://orcid.org/0000-0003-1250-2035>

Albert Wolkerstorfer  <http://orcid.org/0000-0003-1421-1493>

REFERENCES

- Mitragotri S. Current status and future prospects of needle-free liquid jet injectors. *Nat Rev Drug Discov.* 2006;5(7):543–8.
- Barolet D, Benohanian A. Current trends in needle-free jet injection: an update. *Clin Cosmet Investig Dermatol.* 2018;11:231–8.
- Oltulu P, Ince B, Kokbudak N, Findik S, Kilinc F. Measurement of epidermis, dermis, and total skin thicknesses from six different body regions with a new ethical histometric technique. *Turk J Plast Surg.* 2018;26(2):56–61.
- Wanner M, Sakamoto FH, Avram MM, Chan HH, Alam M, Tannous Z, et al. Immediate skin responses to laser and light treatments: Therapeutic endpoints: How to obtain efficacy. *J Am Acad Dermatol.* 2016;74(5):821–33.
- Bik L, van Doorn MBA, Biskup E, Ortner VK, Haedersdal M, Olesen UH. Electronic pneumatic injection-assisted dermal drug delivery visualized by ex vivo confocal microscopy. *Lasers Surg Med.* 2020;53:141–147.
- Erlendsson AM, Haedersdal M, Rossi AM. Needle-free injection assisted drug delivery-histological characterization of cutaneous deposition. *Lasers Surg Med.* 2020;52(1):33–7.
- Simmons JA, Davis J, Thomas J, Lopez J, Le Blanc A, Allison H, et al. Characterization of skin blebs from intradermal jet injection: ex-vivo studies. *J Controlled Release.* 2019;307:200–10.
- Johnson LC, Corah NL. Racial differences in skin resistance. *Science.* 1963;139(3556):766–7.
- Linn L, Boyd B, Iontchev H, King T, Farr SJ. The effects of system parameters on in vivo injection performance of a needle-free injector in human volunteers. *Pharm Res.* 2007;24(8):1501–7.
- Levenberg A, Vinshok Y, Artzi O. Potentials for implementing pressure-controlled jet injection in management of keloids with intralesional 5FU and corticosteroids. *J Cosmet Dermatol.* 2020;19(8):1966–72.
- Agius E, Mooney JM, Bezzina AC, Yu RC. Dermojet delivery of bleomycin for the treatment of recalcitrant plantar warts. *J Dermatolog Treat.* 2006;17(2):112–6.
- Patakfalvi L, Benohanian A. Needle-free anaesthesia, a promising option for the needle-phobic patient. *Br J Dermatol.* 2014;170(5):1191–2.
- Vadeboncoeur S, Richer V, Nantel-Battista M, Benohanian A. Treatment of palmar hyperhidrosis with needle injection versus low-pressure needle-free jet injection of onabotulinumtoxin: an open-label prospective study. *Dermatol Surg.* 2017;43(2):264–9.
- Barolet D, Boucher A. No-needle jet intradermal aminolevulinic acid photodynamic therapy for recurrent nodular basal cell carcinoma of the nose: a case report. *J Skin Cancer.* 2011;2011:790509.
- Naranjo Garcia P, Vinshok Y, Lopez Andriano R, Cohen N. Efficient treatment of upper-lip rhytids by pneumatic administration of hyaluronic acid. *J Cosmet Laser Ther.* 2019;21(6):346–8.
- van den Bemt B, Gettings L, Domańska B, Bruggraber R, Mountian I, Kristensen LE. A portfolio of biologic self-injection devices in rheumatology: how patient involvement in device design can improve treatment experience. *Drug Deliv.* 2019;26(1):384–92.
- McAllister L, Anderson J, Werth K, Cho I, Copeland K, Le Cam Bouveret N, et al. Needle-free jet injection for

- administration of influenza vaccine: a randomised non-inferiority trial. *Lancet*. 2014;384(9944):674–81.
18. Kong X, Luo M, Cai L, Zhang P, Yan R, Hu Y, et al. Needle-free jet injection of insulin glargine improves glycaemic control in patients with type 2 diabetes mellitus: a study based on the flash glucose monitoring system. *Expert Opin Drug Deliv*. 2020
 19. Ruddy BP, Bullen C, Chu JTW, Jeong SH, Madadkhahsalmasi B, McKeage JW, et al. Subcutaneous nicotine delivery via needle-free jet injection: a porcine model. *J Control Release*. 2019;306:83–8.

How to cite this article: Bik L, Doorn MBAv, Boeijink N, Wennekers M, Meesters AA, Bloemen P, et al. Clinical endpoints of needle-free jet injector treatment: an in depth understanding of immediate skin responses. *Lasers Surg Med*. 2022; 1–9. <https://doi.org/10.1002/lsm.23521>